Opt Quant Electron (2013) 45:673–679
DOI 10.1007/s11082-012-9630-8

Optimization for mid-wavelength InSb infrared focal plane arrays under front-side illumination

N. Guo · W. D. Hu · X. S. Chen · W. Lei · Y. Q. Lv · X. L. Zhang · J. J. Si · W. Lu

Received: 28 September 2012 / Accepted: 25 October 2012 / Published online: 10 November 2012

Abstract The quantum efficiency for mid-wavelength InSb infrared focal plane arrays has been numerically studied by two dimensional simulators. Effects of thickness of *p*-type layer on the quantum efficiency under front-side illumination have been obtained. The calculated results can be used to extract the optimal thickness of the *p*-type layer for different absorption and diffusion lengths. It is indicated that the optimal thickness of the *p*-type layer strongly depends on the absorption coefficient and the minority carrier lifetimes. The empirical formulas are also obtained to describe the correlation between the optimal thickness of the *p*-type layer, and the absorption and diffusion lengths.

Keywords InSb Infrared focal plane arrays · Numerical simulation · Quantum efficiency

1 Introduction

InSb, a III-V semiconductor, has a 0.227 eV band gap at 77 K and a cut-off wavelength of 5.5 μm. Due to its excellent absorption ability in the spectral range of 3–5 μm, superior fundamental properties and simple material growth and device fabrication processes, InSb has been widely used for thermal imaging in numerous military and civil fields

N. Guo · W. D. Hu (✉) · X. S. Chen (✉) · W. Lu
National Laboratory for Infrared Physics, Shanghai Institute of Technical Physics, Chinese Academy of Sciences, 500 Yu Tian Road, Shanghai, 200083, China
e-mail: wdhu@mail.sitp.ac.cn

X. S. Chen
e-mail: xschen@mail.sitp.ac.cn

W. Lei
School of Electrical, Electronic and Computer Engineering, University of Western Australia, Crawley, WA 6009, Australia

Y. Q. Lv · X. L. Zhang · J. J. Si
Luoyang Optoelectronic Institute, Luoyang, Henan 471009, China

(Fishman et al. 2007; Shtrichman et al. 2007; Gau et al. 2000; Shen 1994; Parrish et al. 1991; Rogalski 2002; Chang et al. 2006; Kimukin et al. 2003). Generally, for the epitaxial film or bulk material that is subsequently thinned to form an InSb infrared detector, the quantum efficiency (QE) is limited by the characteristics of absorption layer, which are related to the absorption layer thickness, absorption length and diffusion length. Furthermore, crosstalk caused by lateral diffusion of photo-generated carriers can also reduce the spatial resolution of the focal plane arrays (FPAs) and degrade the overall system performance. Therefore, fully understanding the photoresponse mechanisms of InSb and optimizing the device structure to improve the QE are particularly important.

In this paper, two dimensional (2D) simulators are used to calculate the characteristics of InSb FPAs. The effects of p-type layer thickness on the device QE under front-side illumination have been studied. The QE limited by the p-type layer characteristics is theoretically indicated in detail.

2 Device structure and simulation models

The InSb FPAs discussed here are composed of three pixels, as shown in Fig. 1 Timlin and Martin (1993). The n region with a doping density of 10^{15}cm^{-3}, has a thickness of 10μm. The p region is doped with a density of 10^{17}cm^{-3} and its thickness is an adjustable parameter in the simulated process. The assumed values of the doping concentration are from references Fishman et al. (2007) and Treado et al. (1994). In addition, the pixel pitch and the fill factors are 50 μm and 92% respectively. It should be noted that each element including an individual $p-n$ junction forms an island on the 20-μm-thick silicon substrate. Usually, the silicon substrate with a thickness of several tens or hundreds micrometers has to be sufficiently thick to be mechanically robust. However, in our simulation, the silicon substrate is transparent to the incident infrared optical energy. In order to lower the consumptions of time and memory on calculations, the 20 μm thin substrate is assumed. A metal grid layer positioned between the p region and the silicon substrate is used to connect every p region to a reference potential level. And the Indium columns or bumps deposited on the top of n regions connect the readout integrated circuit system. The details about the specific process are given in Timlin et al.

During the simulation, only the center pixel is front-side illuminated, i.e., the optical energy is incident on the p region. Finally the QE curve from pixel 2 is obtained. Meanwhile, the crosstalk, which is defined as a percentage corresponding to the response of pixel 1 divided by the response of pixel 2 (Musca et al. 1999; Bloom and Nemirovsky 1991), can be evaluated by computing the photocurrent at the contacts. In this simulation, for simplicity,

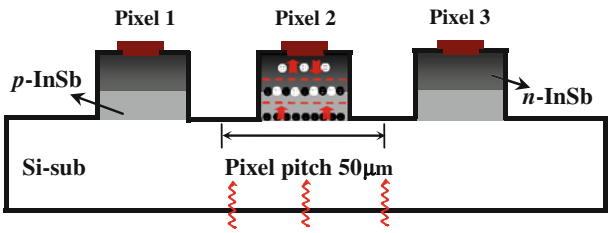

Fig. 1 Schematic of InSb infrared focal plane arrays. The arrows in pixel2 mark the direction of carrier diffusion ("-" represents electron and "+" represents hole). And the area between the dashed lines is the $p-n$ junction

Table 1 List of the key parameters used in the simulation

$E_g = 0.227$	eV	Band gap at 77K
$T = 77$	K	FPA temperature
$\varepsilon = 16.8$		Dielectric constant
τ_n	s	Electrons lifetime (adjustable parameter)
$\tau_p = 10^{-6}$	s	Holes lifetime
$\lambda = 5$	μm	Wavelength
$D_n = \mu_n(kT/q) = 266$	cm^2/s	Electron diffusion coefficient
$D_p = \mu_p(kT/q) = 66$	cm^2/s	Hole diffusion coefficient
$L_n = (\sqrt{D_n \tau_n})$	μm	Electron diffusion length
$L_p = (\sqrt{D_p \tau_p}) = 81.2$	μm	Hole diffusion length
$P = 10^{-4}$	W/cm^{-2}	Wave power

the effect of anti-reflective coatings is not taken into consideration, and this will make the device QE lower than that of experiment (Treado et al. 1994).

In this paper, numerical simulations are performed using Sentaurus Device, a commercial package by Synopsys. The model used here is based on drift-diffusion method, where the well-known Poisson and continuity equations are coupled on the finite element mesh (D'Orsogna et al. 2008). A set of partial differential equations are solved self-consistently on the discrete mesh in an iterative fashion. In order to capture the occurring physical phenomena better, the mesh density around the junctions has also been increased. By default, electrodes are Ohmic electrical boundary conditions, and the incident photon density flux distribution is uniform. The carrier generation-recombination process consists of Shockley-Read-Hall, Auger, and optical generation-recombination terms. Additionally, the tunneling effect, such as indicated in the band-to-band model, is implemented in the continuity equations as additional generation-recombination processes (Guo et al. 2011; Hu et al. 2011, 2010). Key parameters are listed in Table 1.

3 Results and discussion

For the conventional InSb detectors, the infrared radiation is incident on the n-type bulk InSb substrate. The photo-generated minority carriers can diffuse a long distance to $p - n$ junction to be converted into electrical response. However, it is impossible to limit all inter-pixel migration of carriers. Some of them diffuse into neighboring junctions to form the crosstalk (Davis et al. 1998).

In our calculations, all of the diodes are spaced from each other (see Fig. 1). The light is directly incident on the thinner p region instead of n region. The minority carriers generated in the p region can diffuse to the junction more easily with less recombination and, therefore, to lead a higher QE (Davis and Greiner 2011). Moreover, there is still a large amount of optical energy that penetrates through the p region into the junction. Some additional charge carriers are generated to contribute to the enhancement of QE. For longer absorption length (L_a), the n region not far away from the junction can also get some optical energy to produce excess carriers and some of them can diffuse back to the junction (see Fig. 1). For these reasons, there is improved QE in transferring optical energy to electrical energy. So the QE is dependent on not only diffusion length but also absorption length. Additionally, due

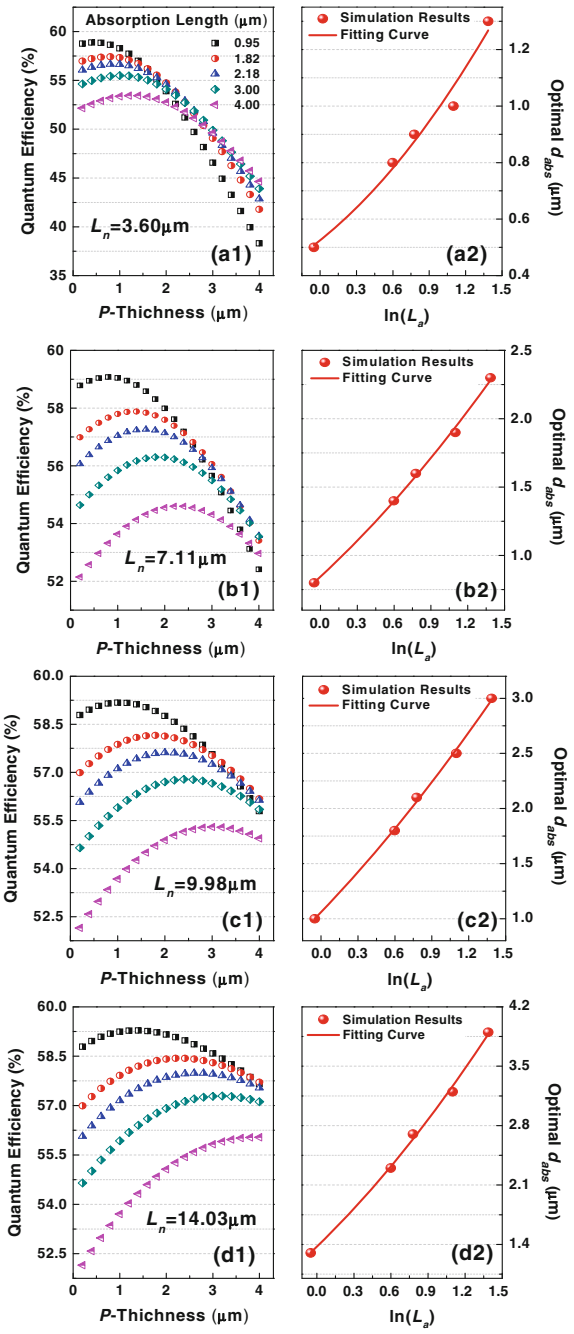

Fig. 2 The QE as a function of p region thickness with L_a changing from 0.95 to 4.0μm for different L_n, i.e., 3.60(a), 7.11(b), 9.98(c), 14.03(d)μm (left column). Fitting curve of the optimum thickness of p region as a function of L_a (right column). "ln" is the Napierian logarithm

to the complete electrical isolation of the diodes, the crosstalk can be reduced significantly. According to our calculation, the crosstalk is about 10^{-6}.

For an actual InSb device under 5 μm irradiation, the carrier lifetime (τ) and the absorption coefficient (α) are constant. Fortunately, the simulation software offers an approach to

Table 2 Fitting coefficients

$L_n(\mu m)$	A	B	C
3.60	0.52	0.34	0.14
7.11	0.84	0.83	0.15
9.98	1.06	1.16	0.16
14.03	1.37	1.41	0.29

change the values of physical parameters for fully understanding the response mechanisms of InSb device. Therefore, in order to find the relation between the optimal thickness of the absorption layer (d_{abs}), i.e. p region, and the absorption layer characteristics, we make some changes on the τ and α. In this simulation, only the electron lifetime τ_n is varied. The reason is that under front-side illumination the radiation is incident on the thinner p region where most optical energy is absorbed and many excess carriers (electrons) are generated. Furthermore, τ_n is usually much shorter than hole lifetime τ_p. The electron diffusion length L_n is more sensitive to the thickness of p region. Figure 2 shows the simulated QE as a function of the p region thickness with L_a changing from 0.95 to 4.0 μm for different L_n, i.e., 3.60, 7.11, 9.98, 14.03 μm (left column). It is found that the shorter L_a can lead to a higher QE and d_{abs} has an increasing trend with L_n changing from 3.60 to 14.03 μm. The results indicate that the complete absorption of optical energy in the p region or near the junction can enhance the device QE. If most incident light is absorbed in n region far away from the junction, the holes as the minority carriers can diffuse not only towards the junction but also in the opposite direction or in a random direction. Thus, the degradation of the device QE may be caused. Moreover, the p region thickness should be shorter than L_n to raise the device QE. By fitting the curve of d_{abs} as a function of L_a (right column), an empirical formula which has the same polynomial format for different L_n is obtained

$$d_{abs} = A + B \times \ln(L_a) + C \times \ln^2(L_a) \tag{1}$$

where A, B, and C are the fitting coefficients, as listed in Table 2 for different L_n.

From Eq. (1) we can find that the optimal thickness of the absorption layer d_{abs} is the function of L_a. However, as mentioned above, the QE is dependent on not only L_a but also L_n. So, in order to deeply explore the influence of L_n on d_{abs}, according to the coefficients listed in Table 2, further calculations have been shown in Fig. 3. And, it can be found that the fitting coefficients A, B, C and L_n meet the following equations well,

$$\begin{aligned} A &= 0.19 + 0.10L_n - 9.80 \times 10^{-4}L_n^2 \\ B &= -0.34 + 0.21L_n - 0.006L_n^2 \\ C &= 2.79 \times 10^{-4}\exp(L_n/2.24) + 0.14 \end{aligned} \tag{2}$$

4 Conclusions

The quantum efficiency of mid-wavelength InSb infrared focal plane arrays has been numerically simulated with a two-dimensional simulator. Compared with the conventional InSb detectors in which only one kind of carriers (electrons) contributes to the response, the device simulated in our work has more complicated carriers (electrons and holes) transporting processes because the front-side illumination and thinner p regions. It is indicated that the absorption length, diffusion length, and the thickness of the $p$region have important role

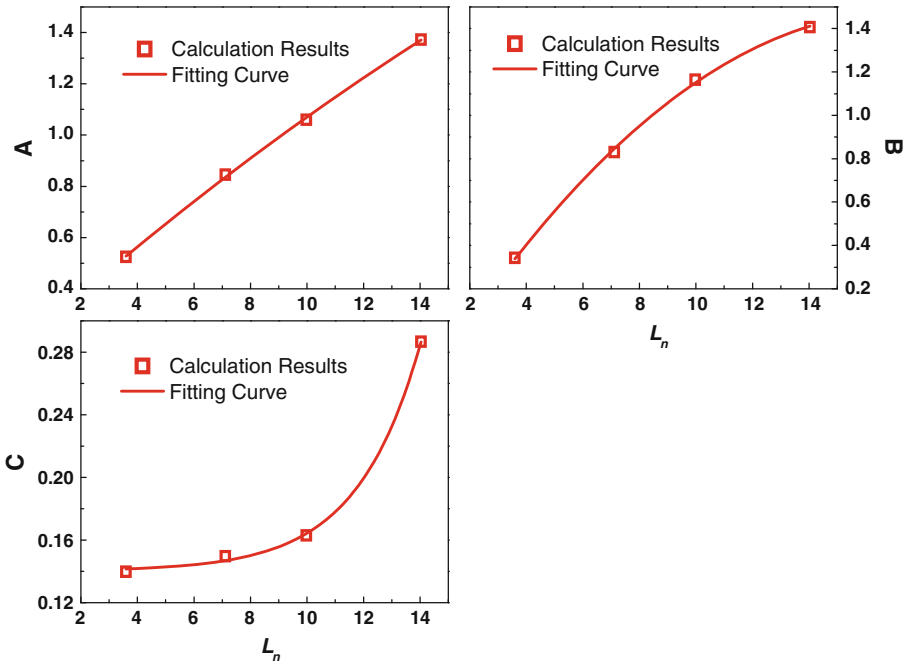

Fig. 3 Fitting curves of coefficients A, B, and C as a function of L_n

in the device quantum efficiency. The optimum thickness of p region and the absorption length is expressed as an empirical formula to design the InSb infrared focal plane arrays with high performance. Furthermore, it is shown that the related fitting coefficients of the empirical formula are strongly dependent on the electron diffusion length.

Acknowledgments The authors thank James Torley from the University of Colorado at Colorado Springs for critical reading of the manuscript. The work was supported by the State Key Program for Basic Research of China (2011CB925604, 2011CB22004), National Natural Science Foundation of China (11274331, 61006090, 61290301, 10990104, 60976092, 61290301), Aviation Science Fund (20110190001), and Shanghai Rising-Star Program.

References

Bloom, I., Nemirovsky, Y.: Quantum efficiency and crosstalk of an improved backside-illuminated indium antimonide focal-plane array. IEEE Trans. Electron Devices **38**, 1792–1796 (1991)

Chang, K.M., Luo, J.J., Chang, C.D., Liu, K.C.: Wet etching characterization of InSb for thermal imaging applications. Jpn. J. Appl. Phys. **45**, 1477–1482 (2006)

D'Orsogna, D., Tobin, S.P., Bellotti, E.: Numerical analysis of a very long-wavelength HgCdTe pixel array for infrared detection. J. Electron. Mater. **37**, 1349–1355 (2008)

Davis, M., Greiner, M.: Indium antimonide large-format detector arrays. Optical Eng. **50**, 061016-1–061016-6 (2011)

Davis, M., Greiner, M., Sanders, J., Wimmers, J.: Resolution issues in InSb focal plane array system design. Proc. SPIE. **3379**, 288–299 (1998)

Fishman, T., Nahum, V., Saguy, E., Calahorra, Z., Shtrichman, I.: 3D simulation of detector parameters for backside illuminated InSb 2-D arrays. Proc. SPIE. **6660**, 666005-1–666005-10 (2007)

Gau, Y.T., Dai, L.K., Yang, S.P., Weng, P.K., Huang, K.S., Liu, Y.N., Chiang, C.D., Jih, F.W., Cherng, Y.T., Chang, H.: 256 × 256 InSb focal plane arrays. Proc. SPIE. **4078**, 467–479 (2000)

Guo, N., Hu, W.D., Chen, X.S., Meng, C., Lv, Y.Q., Lu, W.: Optimization of microlenses for InSb infrared focal-plane arrays. J. Electron. Mater. **40**, 1647–1650 (2011)

Hu, W.D., Chen, X.S., Yin, F., Ye, Z.H., Lin, C., Hu, X.N., Li, Z.F., Lu, W.: Numerical analysis of two-color HgCdTe infrared photovoltaic heterostructure detector. Opt. Quant. Electron. **41**, 699–704 (2010)

Hu, W.D., Chen, X.S., Ye, Z.H., Meng, C., Lv, Y.Q., Lu, W.: Effects of absorption layer characteristic on spectral photoresponse of mid-wavelength InSb photodiodes. Opt. Quant. Electron. **42**, 801–808 (2011)

Kimukin, I., Biyikli, N., Ozbay, E.: InSb high-speed photodetectors grown on GaAs substrate. J. Appl. Phys. **94**, 5414–5416 (2003)

Musca, C.A., Dell, J.M., Faraone, L., Bajaj, J., Pepper, T., Spariosu, K., Blackwell, J., Bruce, C.: Analysis of crosstalk in HgCdTe p-on-n heterojunction photovoltaic infrared sensing arrays. J. Electron. Mater. **28**, 617–623 (1999)

Parrish, W.J., Blackwell, J.D., Kincaid, G.T., Paulson, R.C.: Low-cost high performance InSb 256 $\times$ 256 infrared camera. Proc. SPIE. **1540**, 274–284 (1991)

Rogalski, A.: Infrared detectors: an overview. Infrared Phys. Technol. **43**, 187–210 (2002)

Shtrichman, I., Fishman, T., Mizrahi, U., Nahum, V., Calahorra, Z., Arona, Y.: Spatial resolution of SCD's InSb 2D detector arrays. Proc. SPIE. **6542**, 65423M-1–65423M-11 (2007)

Shen, S.C.: Comparison and competition between MCT and QW structure material for use in IR detectors. Microelectronics J. **25**, 713–739 (1994)

Timlin, H.A., Martin, C.J.: Electro-optical detector array. U.S.Patent No. 5,227,656, (1993)

Treado, P.J., Levin, I.W., Lewis, E.N.: Indium antimonide (InSb) focal plane array (FPA) detection for near-infrared imaging microscopy. Appl. Spectrosc. **48**, 607–615 (1994)